Colloid Polym Sci (2008) 286:1097–1102
DOI 10.1007/s00396-008-1886-y

SHORT COMMUNICATION

Synthesis of high-quality core–shell quantum dots of CdSe–CdS by means of gradual heating in liquid paraffin

Georgi G. Yordanov · Hideyuki Yoshimura · Ceco D. Dushkin

Received: 6 February 2008 / Revised: 17 April 2008 / Accepted: 5 May 2008 / Published online: 31 May 2008

Abstract Here, we report a novel strategy to prepare fluorescent semiconductor quantum dots (QDs) of core–shell type with CdSe–CdS QDs as a model system. Our synthesis was carried out in liquid paraffin, which is a natural, nontoxic, and cheap solvent. We applied a single injection of precursor for the shell growth at low temperature and gradual heating of the reaction mixture after that. By this manner, the Ostwald ripening of the cores was reduced, homogenous nucleation of the shell material was avoided, and highly monodisperse in size core–shell QDs were prepared. Our synthesis method allows working on open air; it is relatively fast and allows fine control over the shell growth process. It leads to the formation of core–shell CdSe–CdS QDs with fluorescence quantum yield as high as 65%. We described the optical properties of core–shell QDs by the model of attenuated quantum confinement.

Keywords CdSe · CdS · CdSe–CdS · Core–shell · Nanoparticles · Nanocrystals · Quantum dots · Fluorescence · Attenuated quantum confinement

Electronic supplementary material The online version of this article (doi:10.1007/s00396-008-1886-y) contains supplementary material, which is available to authorized users.

G. G. Yordanov · C. D. Dushkin (✉)
Laboratory of Nanoparticle Science and Technology, Department of General and Inorganic Chemistry, Faculty of Chemistry, University of Sofia,
1 James Boucher Blvd.,
Sofia 1164, Bulgaria
e-mail: nhtd@wmail.chem.uni-sofia.bg

H. Yoshimura
Department of Physics, Meiji University,
1-1-1 Higashimita, Tama-ku, Kawasaki,
214-8571 Kanagawa, Japan

Introduction

Semiconductor nanocrystals, known as quantum dots (QDs), are of great fundamental and industrial interest due to their size-dependent optical properties [1, 2]. For many purposes, such as fluorescent biological labeling [3, 4], core–shell semiconductor nanocrystals are of critical importance. Usually, the shell possesses a higher band gap than the core material [5–7]. In this case, the photo-generated electron and hole inside the nanocrystal will be mostly confined in the core. Consequently, such core–shell nanocrystals typically show bright photoluminescence (PL) [8] and are more stable against photooxidation due to the shell protective role [9]. For example, the PL quantum yield (QY) of core–shell nanocrystals can be as high as 50–80% [8, 10]. The quality of core–shell nanocrystals has not yet reached that of core nanocrystals in terms of size and size distribution control [5–8, 10]. Two issues were stated previously [5] to be critical for maintaining the size distribution of nanocrystals during the growth of shell materials: (1) the elimination of the homogeneous nucleation of the shell materials and (2) the homogeneous monolayer growth of shell precursors onto all core nanocrystals in the solution, yielding shell layers with nearly the same thickness around each core nanocrystal.

Here, we demonstrate a successful solution for these problems. Our synthesis of core–shell QDs is carried out in liquid paraffin, which is a natural, nontoxic, and cheap solvent. We apply a single injection of precursor for the shell growth at low temperature and gradual heating of the reaction mixture after that. By this manner, the Ostwald ripening of the cores is decreased, the homogenous nucleation of the shell material is avoided, and highly monodisperse in size core–shell QDs are prepared. Our synthesis method allows working on open air (no need of Schlenk lines); it is relatively fast and allows fine control over the shell growth process. It leads to

the formation of core–shell QDs of CdSe–CdS with fluorescence QY as high as 65%. Finally, we demonstrate the validity of attenuated quantum confinement [11] to describe the optical properties of core–shell QDs as well.

Experimental procedures

Chemicals

Cadmium oxide (CdO, 99%), sulfur (S, purum, 99.5%), Rhodamine 6G (for fluorescence), and pulverized selenium (Se, pure, 99.5%) were from Fluka. Tributylphosphine (TBP, 97%) was from Aldrich. Liquid paraffin and stearic acid were from RA.M.Oil SpA (Italy) and Hatkim SA (Turkey), respectively. Chloroform was of analytical reagent grade from Labscan Ltd. (Ireland). Toluene, chloroform, methanol, and acetone were purified by distillation. All other chemicals and solvents were used as received, without additional purification. Tributylphosphine sulfide (TBP-S) solution (0.125 M) was prepared by reaction of sulfur (40 mg, 1.25 mmol) and TBP (0.34 ml, 1.35 mmol) and then dilution with liquid paraffin (10 ml). Tributylphosphine selenide (TBP-Se) solution (0.125 M) was prepared by dissolving selenium (100 mg) powder in TBP (0.5 ml) and then diluted with liquid paraffin (9.5 ml). We found that TBP from Fluka (85%) leads to more reactive TBP-chalcogenides than TBP from Aldrich (97%). The synthesis of QDs works with both, but this difference in reactivity must be taken into account in quantitative studies of the growth kinetics.

Synthesis of CdSe QDs

The synthesis of CdSe QDs was carried out according to previously described procedure [12]. Briefly, CdO (50 mg, 0.39 mmol), stearic acid (0.600 g, 2.1 mmol), and liquid paraffin (15 ml) were heated up to ~260°C to obtain a clear solution of cadmium stearate. The solution of TBP-Se (1.0 ml, 0.125 M) was fast injected at 260°C. The reaction mixture was cooled down by dissolving it in cold toluene (70 ml) 30 s after the injection of TBP-Se. After that, it was kept at room temperature for 3 h until gel-like orange precipitate was formed. The mixture was centrifuged (3,000 rpm; 3 min), and the obtained precipitate was washed twice with pure toluene (20 ml) and pure liquid paraffin (20 ml).

Synthesis of CdSe–CdS QDs

Cadmium oxide (50 mg) was dissolved in stearic acid (600 mg) and liquid paraffin (5 ml) at 180°C in open air and cooled down to 120°C. The orange precipitate containing CdSe QDs (prepared as described in "Synthesis of CdSe QDs") was dispersed in liquid paraffin (10 ml) and was transferred into the solution of cadmium stearate. Immediately after the transfer, 2 ml of 0.125 M TBP-S was injected at 100°C. In another similar experiment, 1 ml of 0.125 M TBP-S was injected instead of 2 ml in order to demonstrate the possibility to control the final nanoparticle size by varying the amount of TBP-S precursor. The reaction temperature was raised from 100 to 250°C within 8–10 min and was kept at 250°C for 5 min. Nitrogen gas can be bubbled through the mixture during heating to remove any residual toluene, introduced with the core QDs. Aliquot samples were taken during the process, in order to trace the shell growth by ultraviolet visible (UV-vis) absorbance and fluorescence spectroscopy, and by high resolution transmission electron microscope (HR-TEM)–energy dispersive spectroscopy (EDS) (0.1 ml aliquot was dispersed in 2 ml of 1 vol.% TBP in toluene). The hot reaction mixture was dissolved in toluene (50 ml) and kept at room temperature for 3 h until gel-like orange-red precipitate formed. The mixture was centrifuged (3,000 rpm; 3 min) and the precipitate was washed twice with pure toluene (20 ml). The precipitate was extracted twice with methanol or chloroform solution in order to remove the excess of cadmium stearate, as described in [13]. The as prepared QDs were dissolved in chloroform (50 ml).

Methods for analysis

The absorbance of QDs suspensions was measured by using a UV-vis spectrophotometer Jenway 6400. The fluorescence spectra were measured by using a fluorescence spectrophotometer Cary Eclipse (Varian; excitation at 480 nm). Quartz cuvettes were utilized in both absorbance and emission measurements. The images of nanocrystals were imaged by HR-TEM JEM-2100 F (JEOL) operated at 200 kV of acceleration voltage, equipped with an EDS probe. X-ray diffraction (XRD) spectra were recorded at room temperature on a powder diffractometer (Siemens D500 with CuKα radiation within 2θ range 10–80° and step 0.05° 2θ and counting time 2 s/step).

Fluorescence quantum yield

The relative fluorescence QY of nanoparticles was obtained by comparison with a standard (Rhodamine 6G in ethanol) and using data derived from the fluorescence and the absorbance spectra of QDs as follows (Eq. 1) [14]:

$$\mathrm{QY} = \left(\frac{1 - T_{ST}}{1 - T_X}\right)\left(\frac{\Phi_X}{\Phi_{ST}}\right)\mathrm{QY}_{ST} \tag{1}$$

Here, T_{ST} and T_X are the transmittances at 480 nm for the standard and the sample, respectively, and QY_{ST} is the quantum yield of the standard (95%, excitation at 480 nm

in ethanol solution [15]). The terms Φ_X and Φ_{ST} give the integrated emitted photon flux for the sample and the standard, respectively (excitation at 480 nm). The values of Φ_X and Φ_{ST} are determined from the fluorescence spectra by integrating the emission intensity of the fluorescence band at all other constant conditions. The QY of CdSe and CdSe–CdS were measured in TBP-toluene (1 vol.% of TBP) solution. The absorbance of these solutions was 0.15 at 480 nm. The absorbance of the standard (Rhodamine 6G) solution was also 0.15 at 480 nm. Equal absorbance of the samples at the excitation wavelength is a necessary condition in order to obtain an accurate value for the QY [14].

Results and discussion

Synthesis and characterization of CdSe–CdS QDs

We prepared CdSe QDs in liquid paraffin because it is a natural substance of low price and allows moreover preparation of QDs free from coordinating organics [12]. CdSe QDs, used in our experiments, are spheroids with an average diameter of 3.1 nm (λ_{AB} = 545 nm, λ_{PL} = 560 nm). The full width of the fluorescence band is 43 nm, and the relative QY is 25%. Absorbance and fluorescence spectra are shown in Fig. 1. The XRD profile and TEM image are shown in Figs. 2a and 3a, respectively. The respective size distributions were evaluated from the TEM analysis of 80–120 particles per sample. The XRD spectra were found not suitable for determination of the nanoparticle size by fitting with the Scherrer formula [19] because of impurities (the excess of cadmium stearate) presented in the samples.

We utilized liquid paraffin in the synthesis of CdSe–CdS core–shell QDs as well. In the known procedures, precursors for shell growth are drop-wise added to the solution of QD-cores at relatively high temperature (200–300°C) [5–10]. In our procedure, we injected at once the TBP-S precursor to a solution of CdSe cores and Cd-stearate in paraffin at ~100°C. After the injection, the temperature was gradually raised to 250°C to grow the shell of CdS. The gradual heating, allowed us to prepare core–shell QDs relatively faster by avoiding the Ostwald ripening (dissolution and size defocusing) of CdSe cores at the same time.

Evidence for the CdS shell growth over the CdSe nuclei is the red shifting of absorbance and emission spectra (Fig. 1). TEM confirmed the larger size of core–shell QDs in comparison with the initial CdSe QDs (Fig. 3). Also, the EDS spectrum of CdSe–CdS QDs confirmed the simultaneous presence of cadmium, selenium and sulfur (see the supporting information). The growth of CdS shell starts at temperatures above 200–220°C, as seen from the red shift in Fig. 4. The XRD profiles of the final CdSe–CdS QDs are given in Fig. 2b. The final CdSe–CdS QDs have

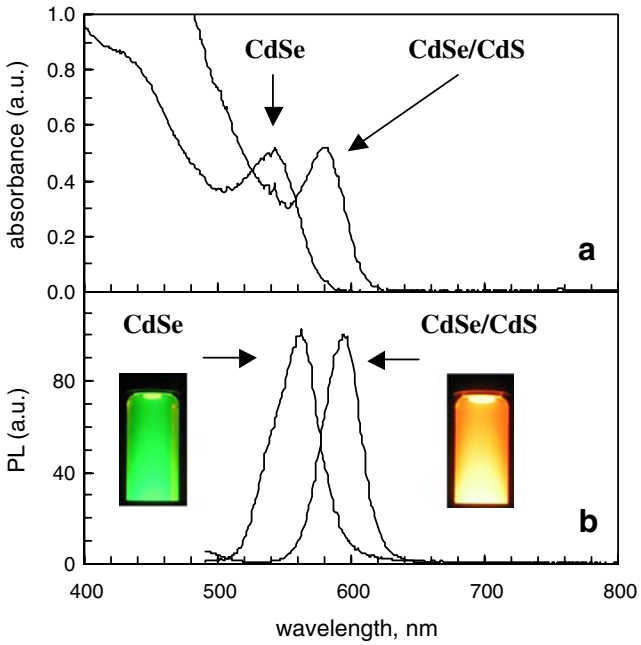

Fig. 1 Normalized (**a**) absorbance and (**b**) fluorescence spectra of the initial CdSe and the final CdSe–CdS QDs synthesized in liquid paraffin. Fluorescence images from the respective QDs in toluene dispersions are shown as *insets* (excitation wavelength 365 nm). (2 ml of 0.128 M TBP-S precursor was used as described in the "Experimental procedures")

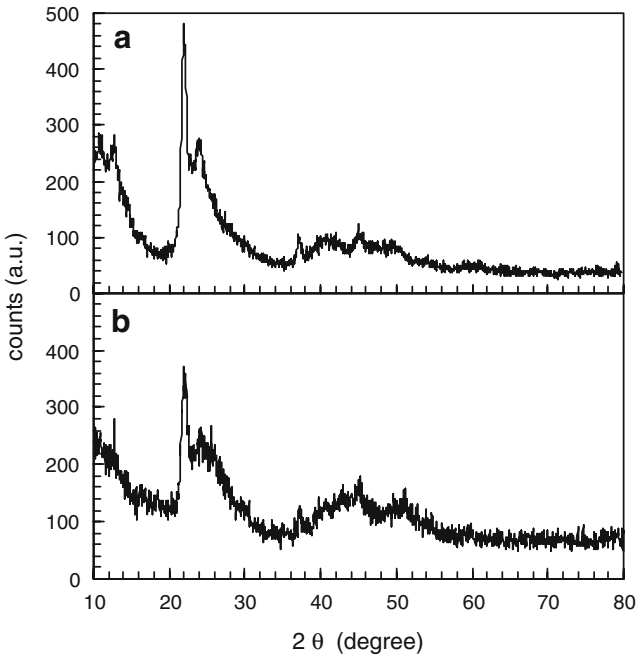

Fig. 2 XRD of (**a**) the initial CdSe and (**b**) the final CdSe–CdS QDs, prepared in liquid paraffin. The sharp peaks at 22° and 38° are from cadmium stearate, which is present in the sample. (2 ml of 0.128 M TBP-S precursor was used as described in the "Experimental procedures")

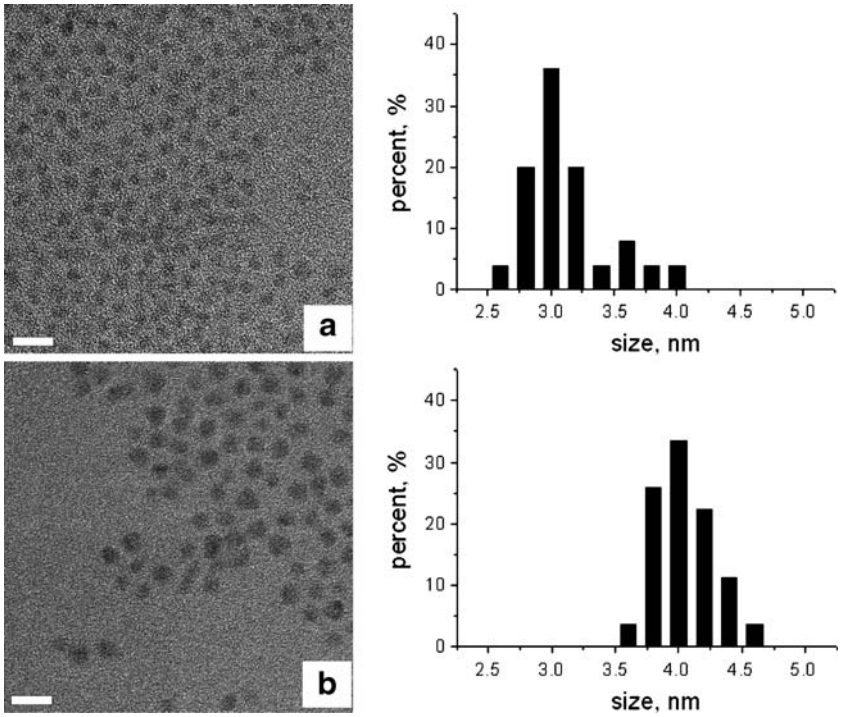

Fig. 3 TEM images (*left panel*) and respective size distributions (*right panel*) of (**a**) the initial CdSe QDs (λ_{AB}=545 nm); (**b**) the final CdSe–CdS QDs (λ_{AB}= 580 nm). (2 ml of 0.128 M TBP-S precursor was used as described in the "Experimental procedures"). Size bars on the TEM images represent 10 nm

narrower emission (the full width of fluorescence band is 33 nm) than the respective CdSe cores. The relative quantum yield for CdSe–CdS QDs (with maximum absorbance and emission wavelengths 580 and 595 nm, respectively) is 65% (note that the QY of CdSe–CdS is much higher than the one for CdSe QDs). A TEM image and size distribution of these CdSe–CdS QDs is shown in Fig. 4b. The average diameter of the final core–shell nanoparticles is 4.1 nm. The PL spectrum of core–shell nanocrystals with very thick shells typically had a shoulder on the high-energy side. TEM studies indicate that the shoulder is not likely caused by a bimodal size distribution. Although, this high-energy shoulder in the PL spectrum was previously also observed [5], its nature is still unclear and needs further study. Possibly, this shoulder could be related to exciton localization in both core and shell materials of CdSe–CdS QDs with a thick CdS shell (see below).

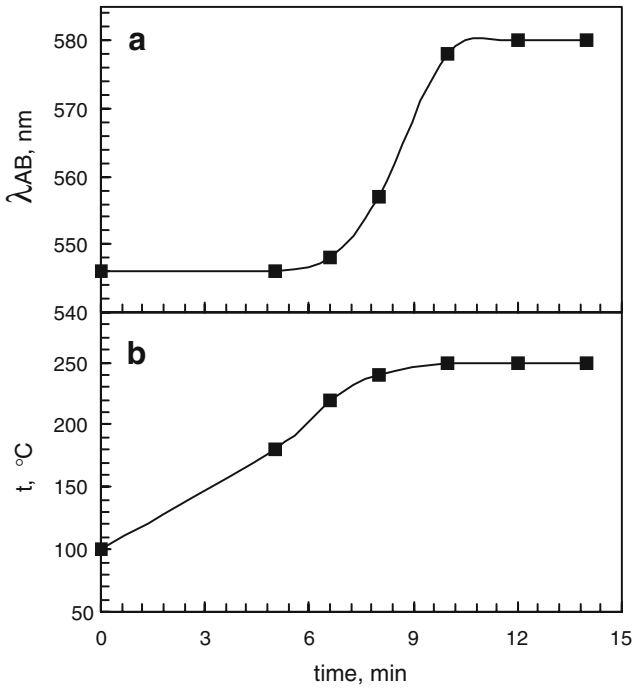

Fig. 4 **a** Red-shifting of exciton absorption peak (λ_{AB}) during the growth of CdS shell over CdSe cores (2 ml of 0.128 M TBP-S precursor was used as described in the "Experimental procedures"); **b** temperature profile of the gradual heating during the CdS shell growth. One can see that the CdS shell starts to grow at temperatures above 200 °C

The final size of the CdSe–CdS core–shell nanoparticles can be controlled in two different ways: by controlling the size of the initial CdSe nuclei and/or by controlling the amount of precursors for the shell growth. In our experiments, the Cd precursor (cadmium stearate) for the shell growth is in excess, and its amount was kept constant. Here, we demonstrate a successful control of the final CdSe–CdS nanoparticle size by varying the amount of TBP-S precursor for the CdS shell growth. For example, starting with the same in size CdSe nuclei, but utilizing different amounts of TBP-S precursor (see the "Experimental procedures"), resulted in different sized final CdSe–CdS core–shell QDs. Thus, doubling the amount of TBP-S precursor results in thicker CdS shell and, thus, larger CdSe–CdS QDs, possessing more red-shifted exciton absorbance and fluorescence spectra (Fig. 5).

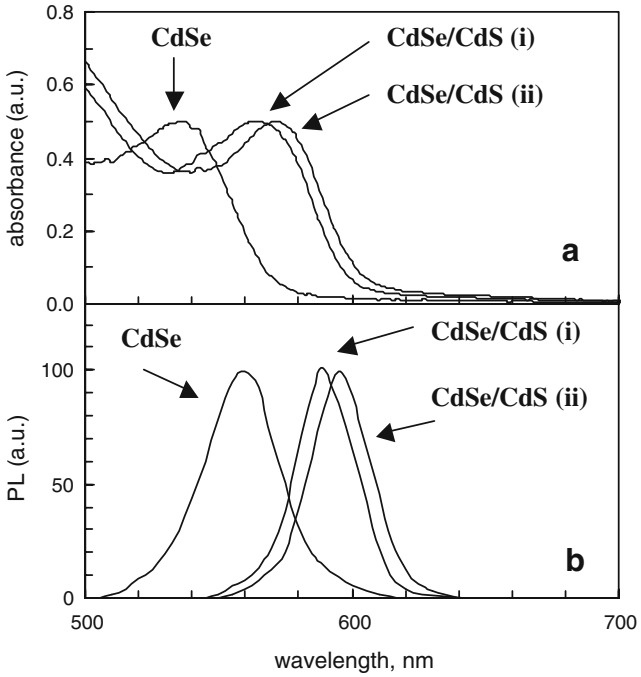

Fig. 5 **a** Absorbance and **b** fluorescence spectra of the initial CdSe nuclei and the final CdSe–CdS core-shell QDs, where different amounts of TBP-S precursor were utilized: (*i*) 1 ml and (*ii*) 2 ml of 0.128 M TBP-S as described in the "Experimental procedures". The temperature profiles during the CdS shell growth was similar the one shown in Fig. 4b

The synthesis of core–shell nanocrystals is a typical example for heterogeneous nucleation and growth of a new phase at the interface between the core nanocrystal and reaction solution. Matching of crystal lattice parameters between the semiconductors is required for a successful shell growth. A heterogeneous nucleating agent provides a lower barrier to the initial formation of the new phase [16]. Thus, the heterogeneous nucleation is expected to occur at lower supersaturation with monomers compared with homogeneous nucleation. We utilized this principle in the design of core–shell nanocrystals synthesis described above. The injection of shell precursor (TBP-S) at low temperature (100°C) does not lead to the formation of shell material because the reaction rate at this temperature is very slow. Raising the temperature leads to increasing of the reaction rate, and shell monomers start to form in the reaction medium. The supersaturation of shell monomers becomes high enough for starting of the heterogeneous nucleation. At this moment, the gradual heating rate is decreased until the shell precursor is consumed in the shell growth. This procedure minimizes the possibilities to induce homogeneous nucleation of shell material. Also, the long-term heating of initial cores is avoided, which decreases the Ostwald ripening and size defocusing. In general, the heterogeneous nucleation depends on the specific nature of the materials involved, but this process is virtually unknown [16].

Table 1 Model parameters for QDs used in the AQC-model

Semiconductor	E_g (eV)	m_1/m_0[a]	l (nm)
CdS	2.4 [18]	0.136 [18]	0.98
CdSe	1.74 [18]	0.107 [18]	0.98

[a] Take relatively to the electron mass, $m_0=9.11\times10^{-31}$ kg

Attenuated quantum confinement

Simple analytical expression based on attenuated quantum confinement (AQC) model has been previously proposed to describe the absorbance spectra of quantum dots [11]. The AQC model is based on the effective mass approximation. The result of AQC model is an energy expression accounting for the degree of exciton penetration outside the nanocrystal core, which is in a very good agreement with experimental data. It allows calculating the true nanocrystal radius from absorption energy by knowing one more parameter of the system—the exciton penetration depth l [11].

We applied the AQC model to derive a simple analytical expression, which describes the red shift of the absorbance spectra during the shell growth. For simplicity of calculations, we used only the expression for the quantum confinement energy term (Eq. 2):

$$E(R) = E_g + \frac{\pi^2\hbar^2}{2m_1(R+l)^2} \tag{2}$$

Here, $E(R)$ is the energy of the lowest excited state, E_g is the energy band gap for bulk semiconductor, $\hbar$ is Planck's constant, m_1 is effective mass of the exciton, R is radius of nanocrystal, and l is the penetration depth of the exciton outside the nanocrystal core.

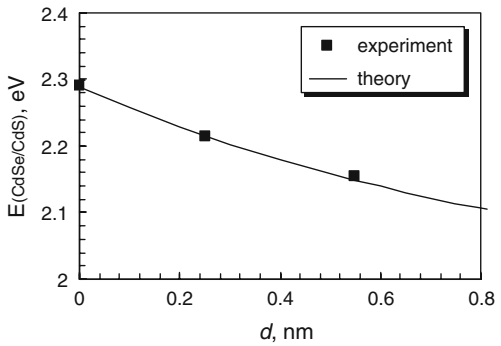

Fig. 6 Attenuated quantum confinement (AQC) model, applied for the case of CdSe–CdS QDs with an initial core (CdSe) size of 3.1 nm. The theoretical curve is calculated by using Eq. 4

For core–shell CdSe–CdS QDs AQC could be written in the superposition form (Eq. 3):

$$E_{\mathrm{CdSe/CdS}} = E_{\mathrm{CdSe}}(R, l_{\mathrm{CdSe}}) + E_{\mathrm{CdS}}(R + d, l_{\mathrm{CdS}}) - E_{\mathrm{CdS}}(R, l_{\mathrm{CdS}}) \quad (3)$$

In Eq. 3, each energy term is represented by a variant of Eq. 2. The resulting expression (Eq. 4) represents the energy of quantum confinement of the exciton in a core–shell quantum dot.

$$E_{CdSe/CdS} = E_g^{\mathrm{CdSe}} + \frac{k_{\mathrm{CdSe}}}{(R + l_{\mathrm{Cdse}})^2} - k_{\mathrm{CdS}}\left[\frac{d(2R + 2l_{\mathrm{CdS}} + d)}{(R + l_{\mathrm{CdS}})^2(R + d + l_{\mathrm{CdS}})^2}\right] \quad (4)$$

Here, d is the thickness of the shell (CdS), and the constant k is expressed by: $k = \pi^2\hbar^2/2m_1$. To obtain values for l_{CdSe} and l_{CdS}, we fitted the experimental curves for CdSe and CdS QDs provided by Yu et al. [17] using Eq. 2 and constants listed in Table 1. We found that the value 0.98 nm for both l_{CdSe} and l_{CdS} fits well the experimental data.

The energy of quantum confinement in core–shell QDs was calculated with Eq. 4 by using the respective parameters from Table 1. The calculated values for the exciton energy are very close to the experimental ones (Fig. 6). As seen, Eq. 4 gives quite accurate results for the exciton energy of core–shell QDs and can be used as a simple analytical expression for approximate calculations.

Conclusions

We describe a simple synthesis of core–shell CdSe–CdS QDs in liquid paraffin by means of gradual heating of the reaction mixture. This synthesis is relatively fast, does not require working in airless conditions and allows a fine control of the shell growth process. The obtained CdSe–CdS QDs are relatively monodisperse in size and have high fluorescence QY. The shift of absorbance spectra of CdSe–CdS QDs to longer wavelengths during the CdS shell growth can be satisfactorily calculated by using a simple analytical expression based on the attenuated quantum confinement.

Acknowledgements The financial support of the Bulgarian Ministry of Education and Science (Project VUH-09/05) is acknowledged. The partial support from the University of Sofia (Project 016/2007 and Project 089/2008) is also acknowledged. G.Y. and C.D. are thankful also to COST Action D43 (grant COST-STSM-D43-02662).

References

1. Yoffe AD (1993) Adv In Phys 42(2):173–266
2. Gaponenko SV (2005) Optical properties of semiconductor nanocrystals. Cambridge University Press, Cambridge
3. Chan W, Nie S (1998) Science 281:2016–2018
4. Bruchez M, Moronne M, Gin P, Weiss S, Alivisatos AP (1998) Science 281:2013–2016
5. Li J, Wang Y, Guo W, Keay J, Mishima T, Johnson M, Peng X (2003) J Am Chem Soc 125:12567–12575
6. Chang JY, Wang SR, Yang CH (2007) Nanotechnology 18:345602
7. Steckel J, Zimmer J, Coe-Sullivan S, Stott N, Bulovic V, Bawendi M (2004) Angew Chem Int Ed 43:2154–2158
8. Hines MA, Guyot-Sionnest P (1996) J Phys Chem 100:468–470
9. Peng X, Schlamp MC, Kadavanich AV, Alivisatos AP (1997) J Am Chem Soc 119:7019–7029
10. Reiss P, Bleuse J, Pron A (2002) Nano Lett 2:781–784
11. Dushkin C, Papazova K, Dushkina N, Adachi E (2005) Colloid Polym Sci 284:80–85
12. Yordanov G, Dushkin C, Gicheva G, Bochev B, Adachi E (2005) Colloid Polym Sci 284:229–232
13. Yu WW, Peng XG (2002) Angew Chem Int Ed 41:2368–2371
14. de Mello Donega C, Hickey SG, Wuister SF, Vanmaekelbergh D, Meijerink A (2003) J Phys Chem B 107:489–496
15. Du H, Fuh RA, Li J, Corkan A, Lindsey JS (1998) Photochem Photobiol 68:141–142
16. Jackson KA (2004) Kinetic processes. Wiley, Weinheim, pp 175–202
17. Yu W, Qu L, Guo W, Peng X (2003) Chem Mater 15:2854–2860
18. CRC (1996) CRC Handbook of Chemistry and Physics. CRC, Boca Raton
19. Patterson AL (1939) Phys Rev 56:978–982